THE ASTROPHYSICAL JOURNAL, 300:77–92, 1986 January 1

MORPHOLOGICAL SEGREGATION IN THE PISCES-PERSEUS SUPERCLUSTER

RICCARDO GIOVANELLI
Arecibo Observatory, National Astronomy and Ionosphere Center[1]
MARTHA P. HAYNES
National Astronomy and Ionosphere Center; and Astronomy Department, Cornell University
AND
GUIDO L. CHINCARINI
Department of Physics and Astronomy, University of Oklahoma; and European Southern Observatory
Received 1985 April 15; accepted 1985 July 1

ABSTRACT

Evidence for the continuous morphological segregation among galaxies along the entire Hubble sequence is sought for the wide range of galaxian densities represented by the Pisces-Perseus supercluster. The present observational data allow the outlining of the gross structure of the supercluster. To the first order, enhancements in the projected surface density distribution of galaxies are shown to reflect volume density enhancements in the supercluster. The two-point autocorrelation function is computed for various subsets of the galaxy sample. Similar to the results found previously for other samples, early-type galaxies in the Pisces-Perseus region tend to cluster on smaller angular scales than do later types. Furthermore, the correlation function $w(\theta)$ for Sa and Sab galaxies is steeper than that of Sb or Sc galaxies. As is seen in rich clusters and groups, the population fractions of elliptical and S0 galaxies grow with increasing density throughout the supercluster, while the spiral fraction correspondingly decreases. The variation in the population fractions can be traced smoothly to regions of very low galaxian density so that a gradient in the population fraction is evident at nearly all density regimes. Even while the fraction of the total population which are spirals decreases as the galaxian density grows, the relative proportion of Sa and Sab galaxies among the spirals increases, while that of Sbc's and Sc's decreases. Because it is unlikely that currently popular mechanisms for merging and gas removal can account for the observed morphological segregation over the wide range of densities characteristic of the supercluster, the explanation of the distribution of morphological types in this region may place interesting constraints on the relative formation eras of galaxies and the large-scale structures in which they are embedded.

Subject headings: cosmology — galaxies: clustering — galaxies: evolution — galaxies: structure

I. INTRODUCTION

In recent years, the scale on which the universe is perceived to be inhomogeneous, infringing on the cosmological principle, has grown, with the recognition of coherent structures which exceed in size typical clusters of galaxies by factors of 10 or more. The observational properties of the known superclusters have been recently reviewed by Oort (1983). The detailed nature of the distribution of galaxies across such wide ranges of intergalactic density is only now being unraveled, but the consequences of local environment on both galaxy formation and evolution are likely to be dramatic, if not in some cases dominant. If the large-scale structures are primordial rather than the more recent result of secular gravitational clustering, we may ask whether some memory of differing environmental conditions at the time of formation has been retained not only by the topology of the large-scale galaxy distribution, but also by the properties of the individual galaxies themselves.

That elliptical galaxies dominate the cores of rich clusters but are much less populous in the field has been long realized, and the cause of such morphological segregation much speculated. Quantitative analyses (Oemler 1974; Melnick and Sargent 1977; Dressler 1980) have shown that the relative population fractions of elliptical, lenticular (S0) and spiral galaxies in clusters and their peripheries are primarily functions of the local galaxian density, and the relationship is less dependent on cluster morphology and the degree of central concentration. To a large extent, this morphological segregation must reflect the early environmental conditions at the time of galaxy formation (Dressler 1984); for example, the variation with local density of the distribution of flatness among lenticular galaxies found by De Souza, Vettolani, and Chincarini (1985) can hardly be explained by density-dependent evolution. Yet, gas removal mechanisms that secularly affect the evolution of spirals also play a role in reinforcing the segregation characteristics in dense, X-ray emitting cluster cores (Haynes, Giovanelli, and Chincarini 1984; Giovanelli and Haynes 1985). The variation in population fraction with local density has been shown to extend in a uniform manner from the high-density regimes of clusters of galaxies to those of typical groups of galaxies (Bhavsar 1981; De Souza *et al.* 1982; Postman and Geller 1984). Nearby loose groups of galaxies are almost always dominated by spirals (de Vaucouleurs 1975), and only in such cases as the groups around NGC 3607 and NGC 5846, where the local density and velocity dispersion are high, are the central bright galaxies of early morphological type. Do the process (or processes) responsible for morphological segregation act as a continuous function of the galaxian density and perhaps reflect the local environmental conditions at the epoch of galaxy formation?

[1] The National Astronomy and Ionosphere Center is operated by Cornell University under contract with the National Science Foundation.

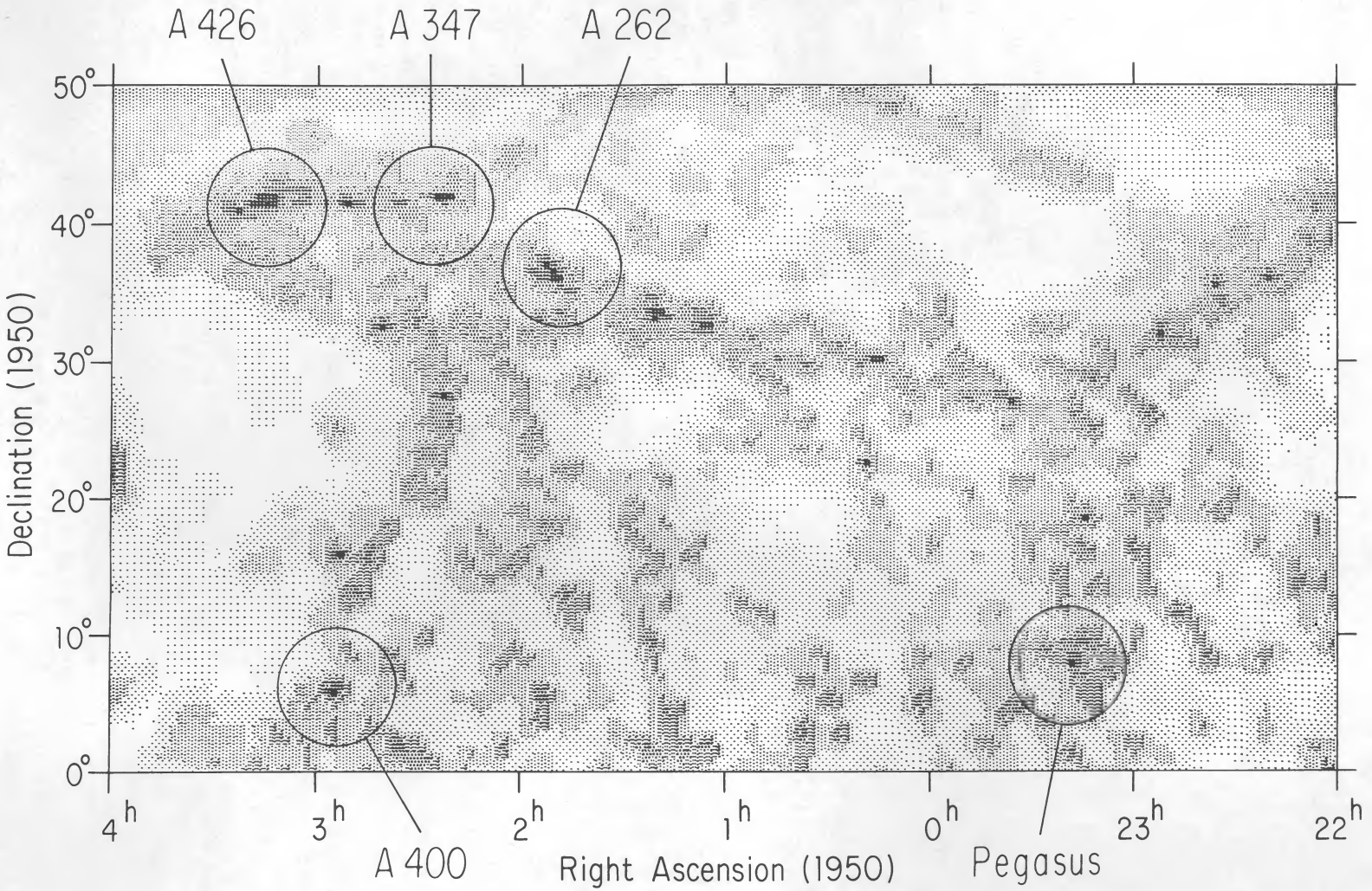

FIG. 1.—Surface density distribution of galaxies in the CGCG after correction for galactic absorption as described in the text. The shade intensity is proportional to the logarithm of the local density parameter. The density scale is arbitrarily normalized to $\sigma = 10$ when the average distance to the 10 nearest galaxies is 1°. The blank regions in the map correspond to $\sigma < 2.2$; the darkest, to $\sigma > 220$. The locations of the major clusters in the Pisces-Perseus supercluster are indicated.

In this paper, we address the latter question by investigating the morphological type distribution in the region of the Pisces-Perseus supercluster. As one of the best examples of large-scale structure in the local universe, the supercluster presents the opportunity to examine the effects of local conditions over a wide range of densities: clusters, groups, filamentary enhancements and the "field." Note that this latter category is best identified as the foreground and background objects. The relative populations of ellipticals, S0's, and spirals vary as predicted by the previous studies. Furthermore, since the great majority of the population outside of the rich clusters consists of spirals, this study can also ask whether systematic segregation exists among the spiral classes themselves.

II. THE DISTRIBUTION OF GALAXIES IN THE PERSEUS REGION

The Perseus supercluster is the major enhancement in the galaxy distribution in the region bounded by $22^h < \text{R.A.} < 4^h$, $0° < \text{decl.} < +50°$. The surface density distribution of galaxies listed in the *Catalog of Galaxies and Clusters of Galaxies* (Zwicky *et al.* 1961–1968, hereafter CGCG) which occupy this region is illustrated in Figure 1. Also indicated are the major clusters in the supercluster. As traced by the curving ridge in Figure 1, the connectivity of the major galaxy groupings in this region was evident even to Bernheimer (1932) who proposed the existence of a "metagalactic cloud" extending from Pegasus to Perseus. More recently, the extent of the supercluster has been discussed by Gregory, Thompson, and Tifft (1981) and by Einasto, Joeveer, and Saar (1981). Over the past several years, we have undertaken a survey of some 3000 spiral galaxies in this region via the 21 cm line of neutral hydrogen. Giovanelli (1983) presented the preliminary results of the largely expanded redshift data base. A first attempt at quantifying the geometry of the supercluster was presented by Chincarini, Giovanelli, and Haynes (1983) who obtained a mean width of about $6h^{-1}$ Mpc and a mean depth of about $12h^{-1}$ Mpc ($h = H_0/100$). Also, Haynes and Giovanelli (1983) have shown that the supercluster includes a widely dispersed population of relatively isolated objects spread throughout the region illustrated in Figure 1 but lying at the same distance as the major features. While a thorough investigation of the three-dimensional distribution of galaxies awaits the completion of our survey, we can already use the existent results to justify the assumption that the large-scale surface density enhancements identifiable in Figure 1 correspond indeed to intensified volume densities.

In order to create Figure 1, the region was divided into 180 by 100 cells, each covering 2^m R.A. and 0°.5 decl. A projected density σ was computed for the position at the center of each cell as the inverse square of the average projected angular distance r_{av} to the 10 nearest galaxies listed in the CGCG, that is, $\sigma \propto 1/r_{av}^2$. Because galactic absorption has an important effect, most dramatic near the northern and eastern boundaries, the density map thus obtained was corrected for extinction. Following Burstein and Heiles (1978), we used absorption corrections derived from the measurements of the galactic H I column density and the Lick survey galaxy counts. Note that the latter survey was of sufficiently great depth that the surface density enhancements of the relatively nearby structures such as Perseus are obliterated. In applying the galactic absorption correction to the observed surface density map, we have been greatly aided by a tape tabulation kindly provided by D. Burstein. Figure 2 illustrates the pattern of galactic absorption in the Pisces-Perseus region. The shade scale increments in units of 0.2 mag. Heavy extinction, in excess of 1 mag, is evident at the low galactic latitudes of the top corners of the map. In addition, a region with peak absorption larger than one magnitude is also present at higher latitudes, between 3^h and 4^h R.A. Much caution in the interpretation of density features in these portions of the map is necessary.

For the simplest models, the counts of galaxies are expected to grow with apparent magnitude as dex (0.6 mag). In fact, computations using a clustered distribution over a large area show that irregularities are smoothed out and that the dex (0.6 mag) law is preserved. The effect of Δm magnitudes of galactic absorption on the number of counts for a catalog complete to a limiting apparent magnitude m_{lim} consists of dimming the galaxies in the interval $(m_{lim} - \Delta m, m_{lim})$ beyond the limit of the catalog. This effect can be accounted for by multiplying the counts in a given bin of apparent magnitude by the factor $g = \text{dex}\,(0.6\,\Delta m)$. The blackest regions in Figure 2 correspond to $g = 10$. Only regions with $g < 3$ will be used in the following analysis.

A galaxy catalog characterized by a limiting magnitude m_{lim} will display as notable surface density enhancements those volume density enhancements that have sizes along the line of sight that are not large in comparison with the "depth" of the catalog and that are local enough to us so that the catalog samples a substantial fraction of the feature's luminosity function. Clumps that are too small compared with the depth of the catalog are washed out by foreground and background objects, unless their density contrast is very large. For this reason, only the richest clusters are conspicuous in the Lick survey counts. As proposed by previous authors, a maze of linear structures connecting the embedded clusters outlines the Perseus supercluster. Our preliminary results (Giovanelli 1983; Chincarini, Giovanelli, and Haynes 1983) indicate that the volume density enhancement peaks at a mean redshift of about 5000 km s^{-1}; velocities in the major dynamical units range from about 3500 km s^{-1} to nearly 10,000 km s^{-1}. The redshift distribution of a magnitude limited sample peaks at a distance (corresponding to the radial velocity V^*) that can be obtained from the relation

$$V^* = 5.248 \times 10^{0.2 m_{lim}} . \quad (1)$$

Note that this relation is independent of the Hubble constant but depends on the choice of the luminosity function (Chincarini 1982). For a limiting magnitude $m_{lim} = +14.9$, the redshift distribution is expected to peak at $V^* = 5000$ km s^{-1}. If a universal luminosity function applies for galaxies, the CGCG best traces volume density enhancements with characteristic sizes between 5 and 20 Mpc if they are located at redshifts of about 5000 km s^{-1}. As an example, Figure 3 shows the surface density contrast expected for a structure of length $l = 5$ Mpc, with a volume density contrast of 100, in a complete catalog with a limiting magnitude of $m_{lim} = +15.7$ (similar to the CGCG). Figure 3 does not imply that the CGCG will manufacture density enhancements at 5000 km s^{-1}, but rather that the CGCG will display best those surface density enhancements that lie at a redshift of about 5000 km s^{-1}, *if such do indeed exist.*

The major ridge of the Pisces-Perseus supercluster is easily visible as the prominent enhancement extending across almost the entire range of right ascension in Figure 1. This feature is emphasized by the jagged contour in Figure 4 (*upper*). Accompanying the surface density distribution, Figure 4 (*lower*) illustrates, in a position-velocity diagram, the redshift distribution

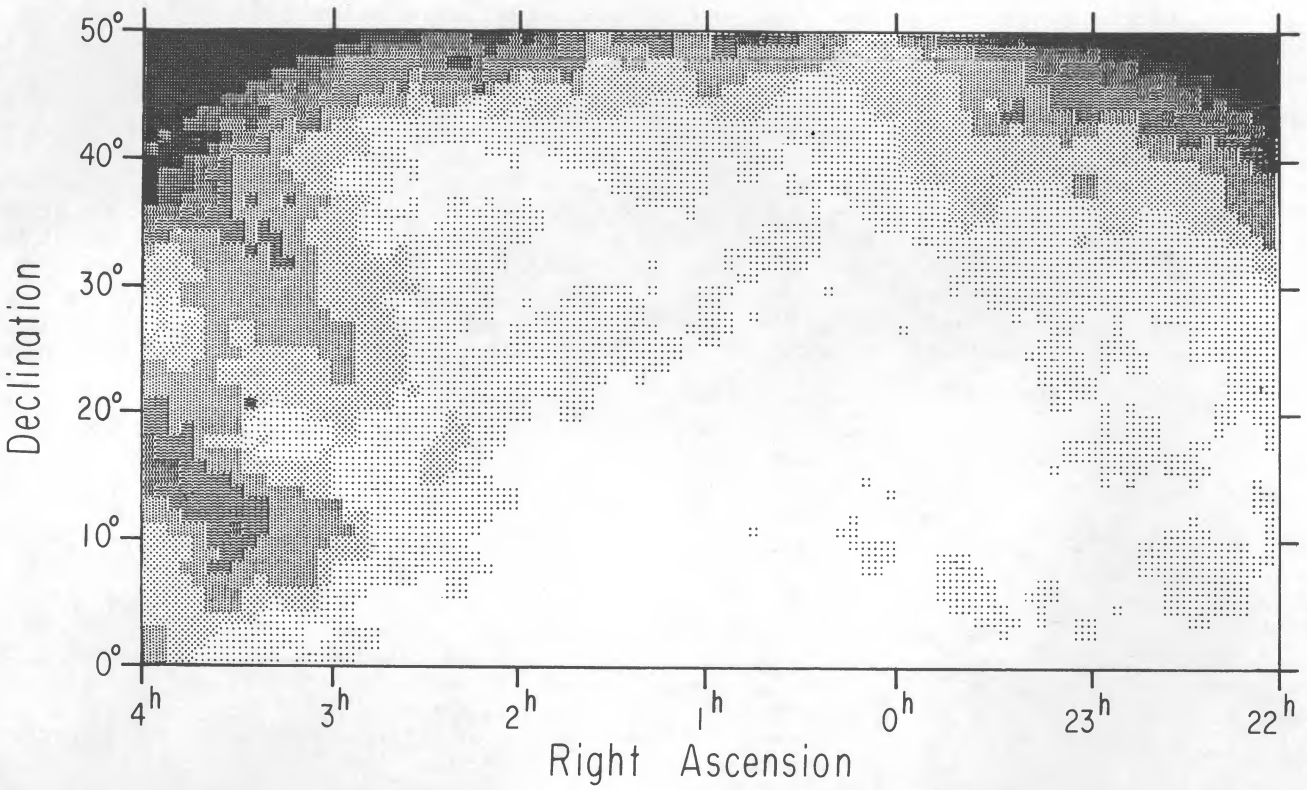

FIG. 2.—Shade plot indicating the map of galactic extinction in the supercluster region. The shade intensity is proportional to the logarithm of the absorption in magnitudes derived following the prescription of Burstein and Heiles (1978), making use of measurements of the galactic H I distribution and the Lick survey galaxy counts. The blank regions correspond to extinction $\Delta m < 0.2$ mag; the darkest, to $\Delta m > 1.4$. The northern corners of the region encounter heavy extinction toward the zone of avoidance.

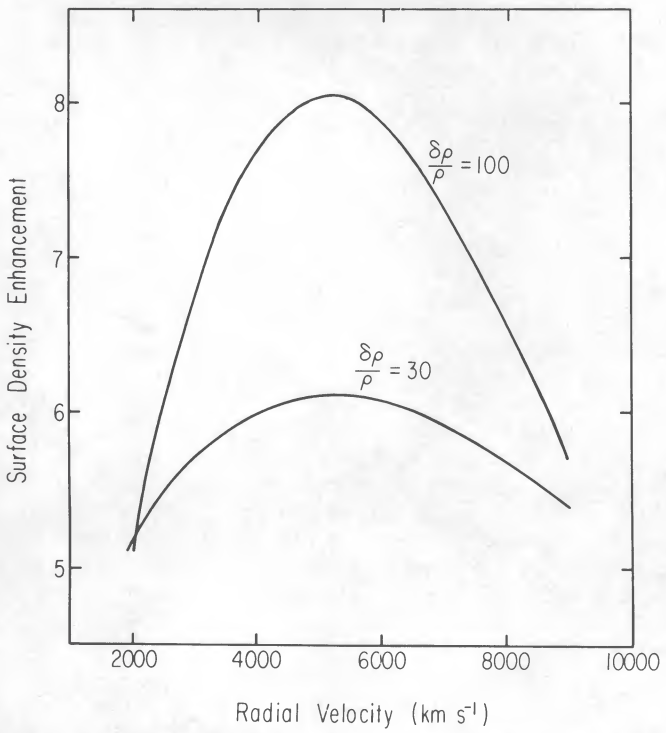

FIG. 3.—Surface density enhancement expected for Gaussian features of half-power linear size $l = 5$ Mpc and characterized by volume density contrasts of 100 and 30 for a catalog complete to a limiting magnitude of +15.7, plotted vs. the enhancement's redshift.

of all galaxies with measured radial velocity that lie within the ridge as outlined in Figure 4 (*upper*). The redshift sample contains 1100 galaxies from our 21 cm redshift survey and from a compilation kindly provided by J. Huchra. It is clear that the impression of connectivity in the two-dimensional distribution is corroborated by the redshift data; the velocity crowding in narrow lanes is striking, occasionally broadening in coincidence with the location of the major clusters characterized by large velocity dispersions. The number of galaxies with known redshift within the outline in Figure 4 (*upper*) is equivalent to about 58% of all galaxies in the *Uppsala General Catalog* (Nilson 1973, hereafter UGC) and about 53% of all CGCG galaxies enclosed in that region. The morphological distribution of galaxies with known redshift is similar to that of a randomly chosen UGC sample. Branching of the ridge into two different velocity regimes is observed near about R.A. = 0^h30^m. Careful inspection shows that the two branches can be followed to trace separate, sometimes intersecting, chains of surface density enhancement.

Figure 5 illustrates the redshift distribution of all galaxies included in Figure 4 (*lower*). The smooth curve superposed on Figure 5 shows the velocity distribution that would have been expected if the observational sample had represented a set of homogeneously distributed objects characterized by a Schechter (1976) luminosity function. The magnitude incompleteness of the observed distribution has been considered in constructing the expected distribution following Giovanelli and Haynes (1982). Because systematic velocity gradients across the ridge have not been removed in compiling Figure 5, the observed histogram at any narrow interval of right ascen-

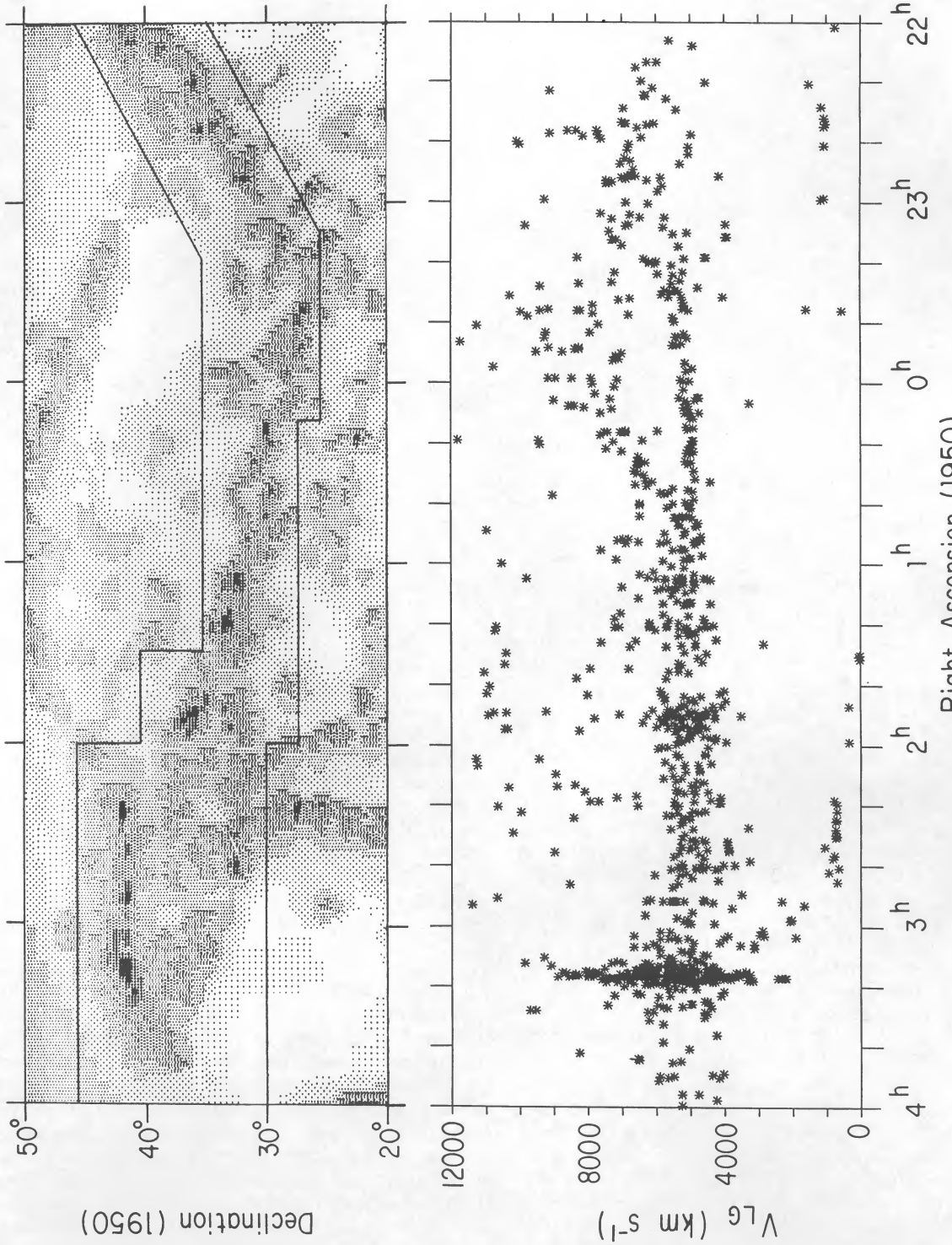

FIG. 4.—Density and velocity distributions along the major ridge of the Pisces-Perseus supercluster. The lower panel shows the velocity distribution as a function of position for galaxies with known redshift which lie within the jagged contour in the upper panel.

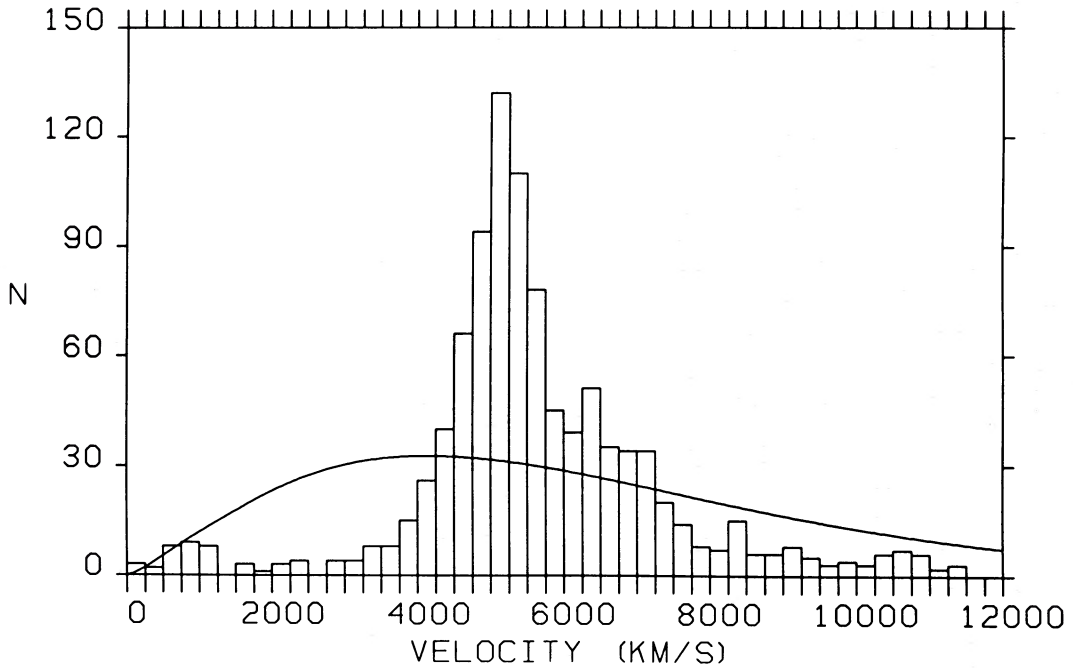

FIG. 5.—Redshift distribution of all galaxies included in Fig. 4 (*lower*). Superposed as the smooth curve is the expected redshift distribution for a sample with the same apparent magnitude distribution as that observed but characterized by a Schechter (1976) luminosity function and populating space homogeneously.

sion would appear sharper than the one displayed. Further velocity broadening is contributed by the large velocity dispersion of the clusters. The difference between such a histogram smoothed in this way and the expected velocity distribution provides clear evidence of confinement in redshift space as well.

Similar analysis, applied to other linear enhancements in Figure 1, indicates that these features also tend to be associated with three-dimensional coherence, although the current degree of completeness of the redshift surveys is somewhat lower towards the southern portions of the region. Two-dimensional filamentary structures have sometimes been referred to as "Martian canals"; with current observational backing, we contend that most of those discernible in Figure 1 do indeed carry water.

An additional interesting detail that derives from inspection of Figure 4 (*lower*) is that, although selection effects play a role in its identification, the main ridge of the Perseus supercluster, rather fortunately, appears to lie at roughly the same distance from us at all points along its length. This favorable aspect provides further reliability for the correspondence between surface and volume densities assumed in the next section.

The question of morphological segregation even within the general category of spiral galaxies in this region can be addressed by examining the distribution of galaxies of differing morphological types in comparison with the total distribution shown in Figure 1. Unfortunately, morphological types are not available for all the galaxies in the CGCG. Rather, the largest set of typed galaxies is that of the UGC; the region included in Figure 1 contains 3558 galaxies classified by Nilson. The UGC inclusion criterion is based on angular size and the catalog is roughly complete for diameters greater than 1′. A caveat: Nilson's morphological classification is widely recognized to be rather good, for work done on PSS prints, and each estimate is qualified by an index; in order to obtain relatively large samples, we have not used Nilson's morphological type quality index as a criterion for selection (this decision was aided by the unavailability to us of a magnetic tape version of the UGC containing such index); thus a margin of uncertainty exists in the type assignments, especially for the smaller angular diameter galaxies. In § IV*c*, we will discuss the biases introduced by our choice of a size-limited catalog to study morphological segregation with respect to the surface densities derived from an apparent magnitude–limited catalog (the CGCG), but it should be noted here that the reasons for such a choice are statistical: the CGCG includes 2000 more galaxies in the Perseus region than does the UGC.

The simplest approach to demonstrating the effects of morphological segregation is displayed in the five panels in Figure 6. Figure 6*a* shows the sky distribution of all galaxies in the UGC contained within the region also included in Figure 1. The other panels show the corresponding distribution of morphological subgroupings of the UGC galaxies. The types included in each subset are indicated in each panel, and all classifications come from the UGC. The ridge of the Perseus supercluster is traced best by the early-type galaxies and is almost invisible among types later than Sc, even though many of those galaxies lie at the same distance from us as does the supercluster. The comparison of the separate distributions give, at a glance, the impression of segregation in higher density regions of galaxies of progressively earlier morphological type, a property that ranges through the spiral classes suggesting a monotonic differentiation of the formation loci with type. An earlier version of these diagrams, including preliminary data from our redshift survey, has been presented by Oort (1983).

In the following sections, we will attempt to quantify the perception suggested by Figure 6 and will discuss the possible biases introduced by systematic differences in the depth—or

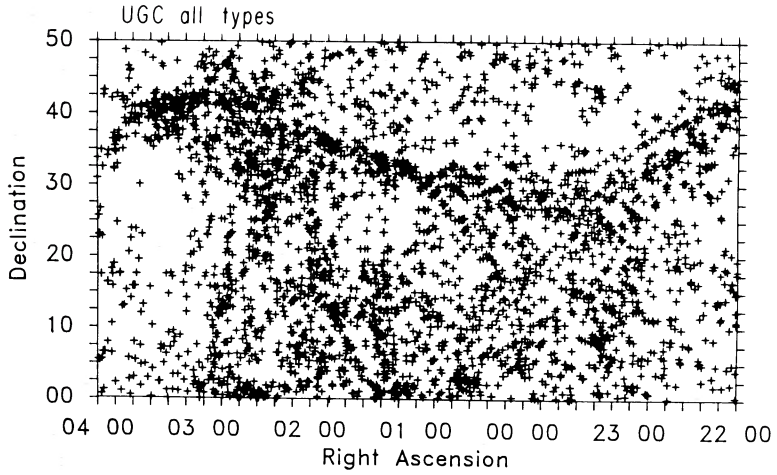

FIG. 6*a*

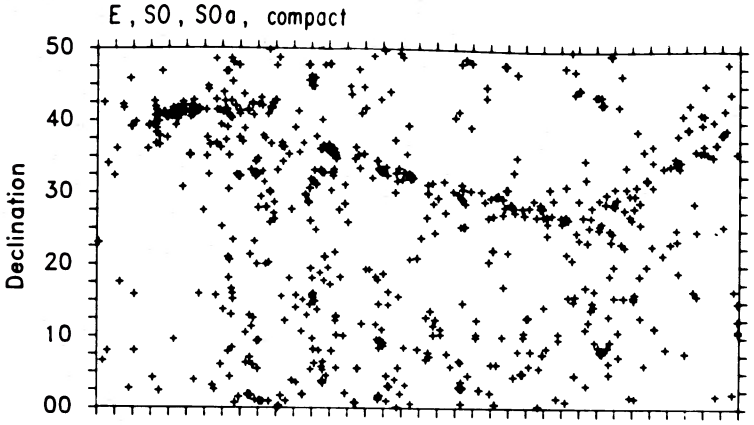

FIG. 6*b*

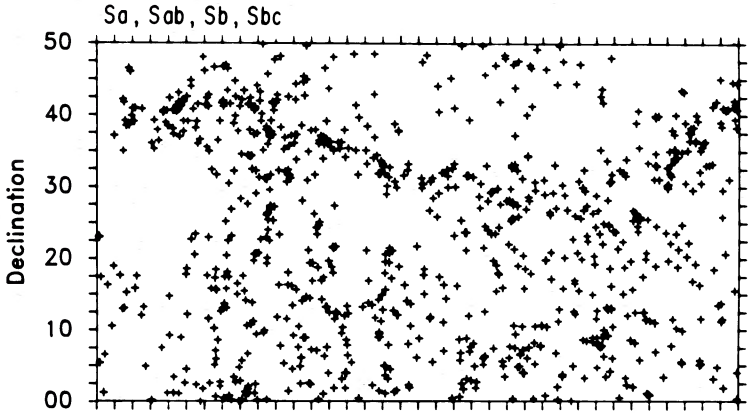

FIG. 6*c*

FIG. 6.—The sky distribution of UGC galaxies of varying morphological type subsets. Figure 6*a* shows the location of all 3558 galaxies in this region which are listed in the UGC. Figures 6*b*–6*e* illustrate the distribution of galaxies of the types indicated in each panel. All classifications come from the UGC via a type coding provided by D. Burstein.

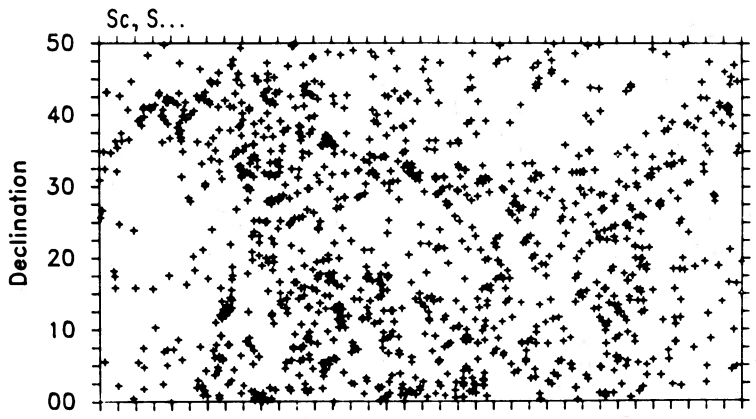

FIG. 6d

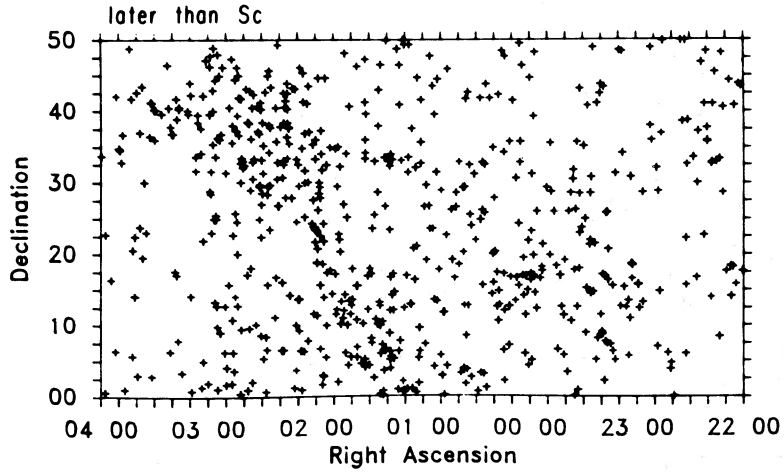

FIG. 6e

redshift distribution—among the subsamples illustrated in Figure 6.

III. TWO-POINT ANGULAR CORRELATION ANALYSIS

A straightforward quantitative approach for analysis of the clustering properties of the galaxian distribution consists of the derivation of the two-point correlation function of a given population (cf. Peebles 1980). Following common practice, we fit our estimate of the two-point angular correlation function with a power law of the form:

$$w(\theta) = A\theta^{\beta} . \quad (2)$$

Davis and Geller (1976) have analyzed the behavior of $w(\theta)$ for various UGC subsamples, separating ellipticals, S0's, and spirals. Here we would like to test whether differences of behavior are discernible among different types within the spiral population in the region of the Perseus supercluster. Our estimates of the correlation function are obtained using a technique described by Hewett (1982), which minimizes the effects of systematic errors introduced by edge effects, variable extinction, etc. Our estimate of the correlation function for a northern galactic cap sample restricted to the magnitude range $m \leq +14.5$, very similar to Sample I of Davis and Geller, yields $A = 0.97 \pm 0.04$, $\beta = -0.69 \pm 0.03$, in close agreement with their results. If the apparent magnitude constraint is relaxed so that all UGC galaxies in the same region are included (a sample about 3.5 times larger), we obtain $A = 1.44$, $\beta = -0.69$.

Figure 7 displays the estimate of $w(\theta)$ for all UGC galaxies in the Perseus region (whose sky distribution is shown in the top panel of Fig. 6*a*). The straight line traces the best-fit power law: $A = 0.71$, $\beta = -0.59$. In comparison, if one limits the sample to the magnitude range $m \leq +14.5$, the value of β remains relatively unchanged, but A triples in size, suggesting that the fainter, typically low surface brightness UGC galaxies in the Perseus supercluster region are much less clumped. Similar results have been obtained by Davis and Djorgovski (1985) who examined the clustering properties of high and low surface brightness objects in the UGC. It is likely that in the Perseus region, at least, these objects are to a large extent representative of a foreground population and therefore show little clustering on angular scales of a few degrees or less.

The estimate of the autocorrelation function of the galaxy distribution $w(\theta)$ shown in Figure 7 has been obtained by subtracting the cross-correlation of the galaxy sample with a random catalog as suggested by Hewett (1982). Galactic obscuration, more important toward the north and east, undoubtedly influences the results to some extent. Note the absence of clumping in the regions of low galactic latitude and very high galactic absorption (see Figs. 1 and 2). If the sample is limited to those galaxies in the region with $23^{h}30^{m} < \text{R.A.} < 02^{h}30^{m}$, $0° < \text{decl.} < +38°$, the best-fit power

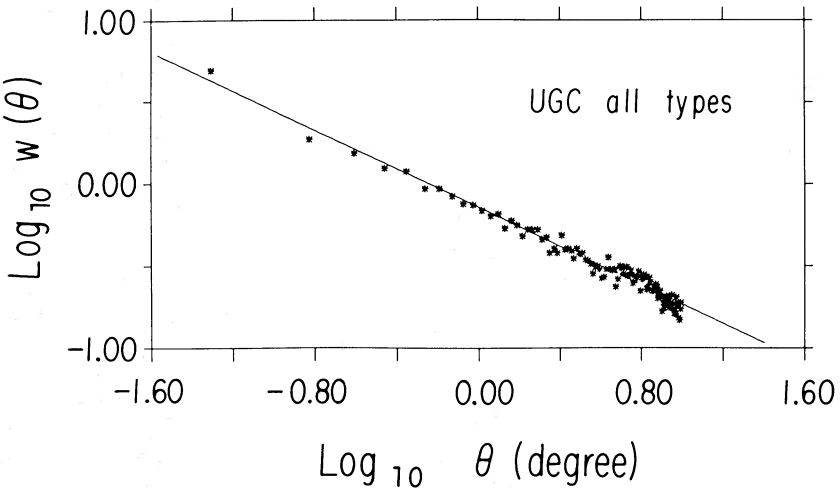

FIG. 7.—Estimate of the two-point angular correlation function $w(\theta)$ for all UGC galaxies contained within the region of the Perseus supercluster. The scale is logarithmic. Corrections have been applied following the method of Hewett (1982). The straight line shows the best-fit power law: $A = 0.71$, $= -0.59$.

law for $w(\theta)$ yields $A = 0.39$ and $\beta = -0.82$. Best-fit parameters for the estimates of $w(\theta)$ obtained for these and the samples described below are included in Table 1.

Figure 8 illustrates the results of the correlation analysis of the Perseus region for six separate subsamples as indicated. Best fits are plotted as the superposed straight lines. In corroboration of the results of Davis and Geller (1976), we find that in the Pisces-Perseus region also, early-type galaxies have steeper correlation functions, with stronger tendencies toward clustering on small angular scales, than do later types. In addition to the comparison among ellipticals, S0's, and spirals, however, the trend continues among the spirals. Late-type spirals (Sb and later) have significantly shallower correlation functions that do Sa's and Sab's. No significant differences appear among spirals of type Sb or later. Figure 9 attempts to solidify this point by combining type subgroups as suggested by Figure 8 in order to improve the statistics. The best-fit estimates of $w(\theta)$ are given in Table 1; spirals of type Sa, Sab, Sb cluster on smaller angular scales than do later spirals, but are not as clumped as ellipticals or S0's. This quantifies the visual impression seen in the lower panels of Figure 6.

IV. POPULATION AS A FUNCTION OF DENSITY

While the two-point correlation analysis is not very sensitive to the presence of large-scale, highly anisotropic, structures such as elongated, one-dimensional filaments, it is nonetheless provoking that the results presented in Table 1 suggest that different clustering behavior characterizes galaxies of different spiral morphology, confirming the visual impressions carried by Figure 6. A further quantitative approach consists of analyzing whether this tendency is also present as a function of local galaxian density. Ideally, we would like to analyze the galaxian population properties for samples that are limited and complete in either absolute magnitude or linear size. While awaiting the completion of redshift surveys that will allow the binning of statistically significant samples in intervals of both local density and morphological type, we adopt a coarser approach, valid for the Perseus region, in which we sample the

TABLE 1

PARAMETERS OF ANGULAR CORRELATION FUNCTION ESTIMATES

Sample (1)	N_{gals} (2)	A (3)	β (4)	Description (5)
1. All	3602	0.71	−0.59	All magnitudes, all types
2. $m < 14.5$	799	2.21	−0.62	Apparent magnitude < 14.5 or less
3. Restricted	1771	0.38	−0.82	23.5 < R.A. < 2.5, 0 < decl. < 38
4. CGCG	5377	0.79	−0.68	
5. Early	725	1.92	−0.90	E, S0, S0a, compact
6. Early spirals	689	0.74	−0.65	Sa, Sab, Sb
7. Late spirals	1548	0.54	−0.37	Sbc and later
8. E	227	2.60	−1.06	E, E–S0
9. S0, S0a	423	1.75	−0.84	
10. Sa, Sab	312	0.29	−0.81	
11. Sb, Sbc	566	0.50	−0.63	
12. Sc	678	0.62	−0.47	
13. Later than Sc	681	0.58	−0.30	S-Irr, Irr, Dw, dm, Sdm, "..."

NOTE.—All samples correspond to the region from 22^h to 04^h in R.A., and from 0° to 50° in decl., and are drawn exclusively from the UGC catalog, except for sample 3, which is restricted to a smaller region (less affected by galactic extinction) and sample 4, which includes all CGCG galaxies in the larger region.

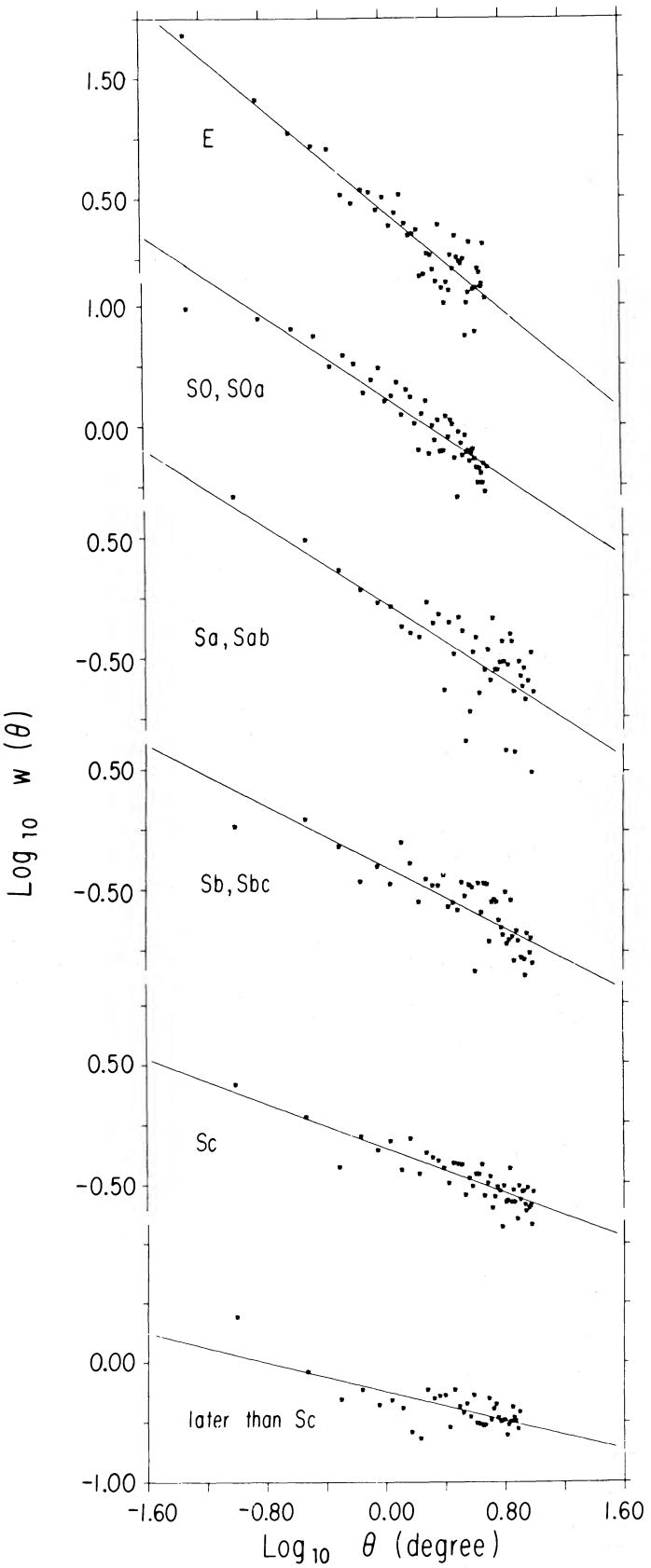

FIG. 8.—Estimate of the two-point angular correlation function $w(\theta)$ vs. (θ), on logarithmic scales, for different morphological subgroups among UGC galaxies in the Pisces-Perseus region. Parameters of the best-fit straight lines are given in Table 1.

TABLE 2

COUNTS OF UGC GALAXIES BY MORPHOLOGICAL TYPE

log σ (1)	E (2)	S0, S0a (3)	Sa, Sab (4)	Sb (5)	Sbc (6)	Sc (7)	S... (8)	Later (9)	All (10)
0.2.....	2	2	4	6	2	14	9	18	64
0.6.....	12	27	20	28	18	63	48	72	305
1.0.....	26	104	55	95	46	197	140	178	922
1.4.....	62	149	118	137	75	242	194	175	1249
1.8.....	54	134	74	73	37	117	86	66	705
2.2.....	42	55	27	28	7	27	17	6	227
2.6.....	19	21	9	5	1	7	5	1	74
>2.8.....	5	3	1	1	0	1	0	0	12

relative distribution of morphological types as a function of the projected surface density. As discussed in § II, the current data map the supercluster sufficiently so that, at least to first order, the surface density enhancements reflect effective volume density enhancements, rather than mere projection effects.

a) The Choice of Catalog

As discussed previously, we employ the morphological type codings given by Nilson in the UGC, but for statistical reasons, the surface densities are computed from the CGCG because it is apparent magnitude limited. In addition to the fact that the CGCG contains 2000 more galaxies in the Perseus region than does the UGC, it is also more straightforward to correct the number counts $n(m)$ for biases introduced by galactic extinction than counts binned by angular size. For comparison, we have also obtained a density array solely for UGC galaxies, as done in order to prepare Figure 1. The density enhancements are similarly located in the two representations; the CGCG, however, enhances density contrasts more than does the UGC, not surprisingly. In § IV*c*, we will discuss the biases introduced by our choice of the CGCG density array.

b) Type Binning and Number Counts

Table 2 lists the counts of UGC galaxies, selected by morphological class, as a function of surface density. In practice, the surface density associated with each galaxy is that computed for the cell within which it is located. As described before, the cell size is 2^m R.A. by 0°.5 decl. and the array of densities consists of 180 by 100 cells in the entire region illustrated in Figure 1. In column (2), we include not only ellipticals, but also those listed as E–S0. Column (3) combines types S0, S0a, and those listed as "... compact"; the latter objects most often reveal lenticular morphology, although a small fraction may be blue and gas-rich and of doubtful parentage with lenticulars. Barred and normal galaxies are not separated, and where compound types are given, such as "Sbc–Sc," the first is adopted. Column (8) contains the nondescript spirals, identified in the UGC as "S", "SB", "S . . . ," etc., while in column (9) we include all galaxies of type later than Sc, the Sd's irregulars, dwarfs, and low-luminosity spirals. Peculiars, multiple systems, and other oddities have not been listed separately, but are included in the compilation of all types in column (10). The counts are binned in steps of 0.4 in log σ, except for those with log $\sigma > 2.8$ which have been accumulated in a single bin.

Figure 10 displays the population fraction of all counts, in each bin of log σ, corresponding to each morphological subgroup. A progressive change is seen in the slope of the variation of population fraction with density, from early to late morphologies. While early-type galaxies appear strongly concentrated toward the regions of highest density, later type

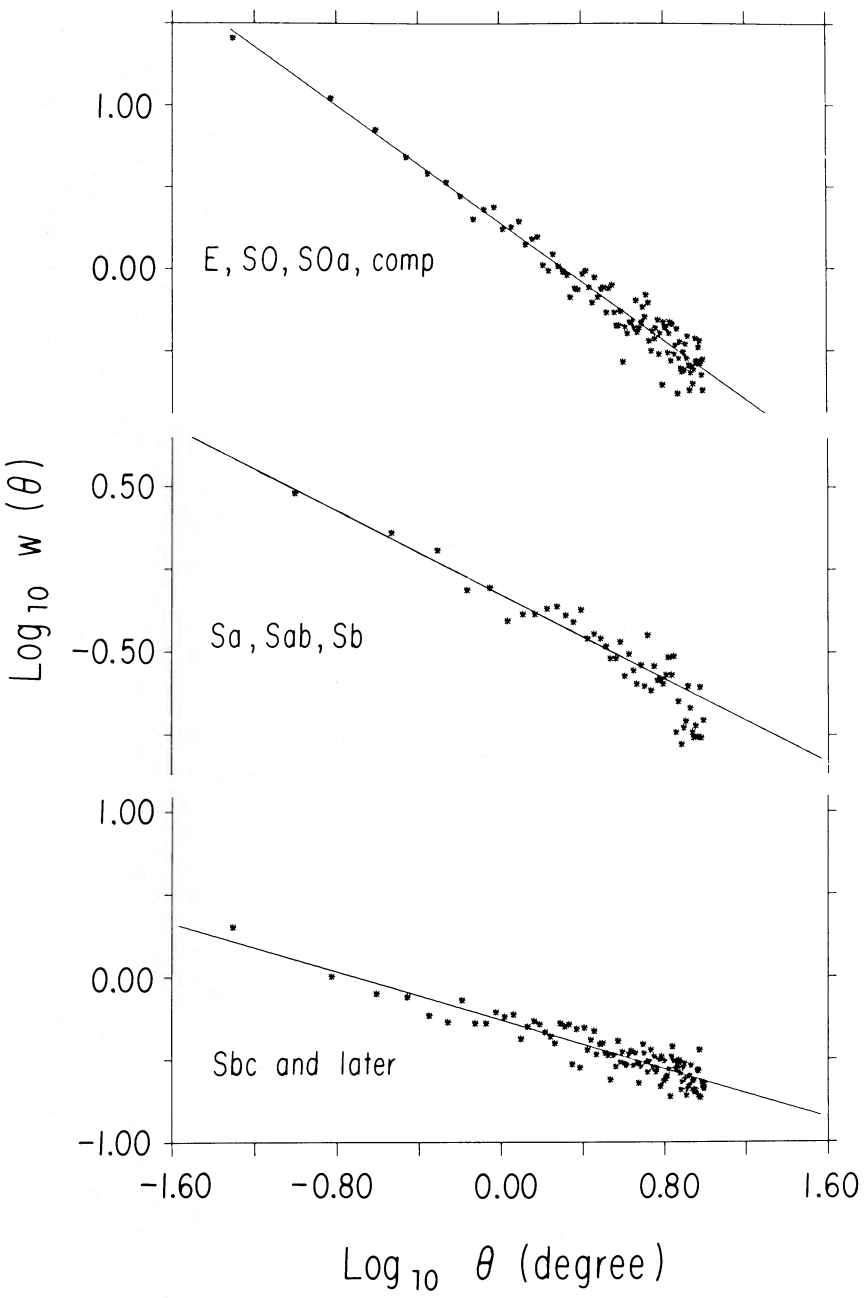

FIG. 9.—Similar to Fig. 8, except that the subgrouping by morphological types has been extended to better the statistics. Types included in each analysis are as indicated. Parameters of the best-fit straight lines are listed in Table 1.

spirals avoid the clusters. This result is in agreement with the well established trend observed in clusters of galaxies (Dressler 1980) and extended to groups by Bhavsar (1981), De Souza *et al.* (1982), and Postman and Geller (1984). Here two details are underscored. First, the trend observed in the cores of clusters and their peripheries appears to continue monotonically to the regions of lowest population density: depending on the choice of morphological class, a gradient in the population fraction of that type alone can be observed at nearly every value of density. Second, the progressive variation in the population fraction, as functions of both density and type, is striking even within the range of spiral morphologies.

When the galaxy population is separated only in terms of the three main categories—ellipticals (E), lenticulars (S0), and spirals plus irregulars (Sp)—the morphological segregation appears to cease at values below log $\sigma = 1.4$, in agreement with the findings of Postman and Geller (1984). At densities lower than that value, the "field" population fractions obtained for the Perseus region sample are, respectively, 0.045, 0.11, and 0.77 for E:S0:Sp. The remaining 7% corresponds to galaxies of peculiar, uncertain, or unspecified morphology; the behavior of this latter class of objects, as a whole, resembles better the spiral rather than the E or S0 population. The "field" population fractions obtained here differ significantly from those obtained for the magnitude-limited samples analyzed by Postman and Geller (who found 0.12:0.23:0.65 and

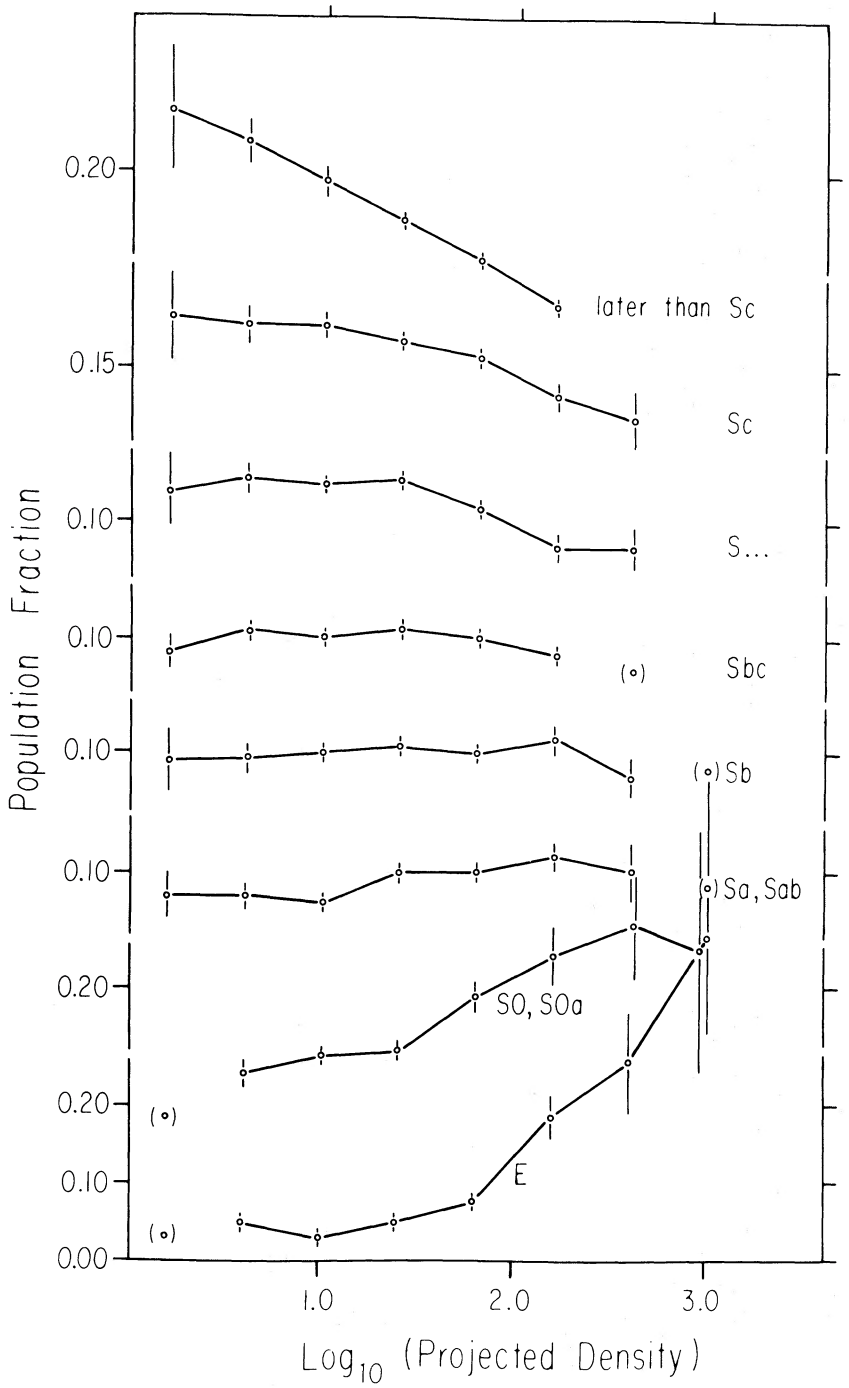

FIG. 10.—Variation of the population fraction with projected surface density on a logarithmic scale for various morphological subgroups for UGC galaxies in the Pisces-Perseus region. The types in each subgroup are as indicated. Error bars are drawn as discussed in the text; points of marginal significance are enclosed in parentheses.

0.11:0.19:0.70 for E:S0:Sp for their CfA and NB samples) and from the field fractions for the *Revised Shapley Ames Catalog* given by Sandage and Tammann (1981) to be 0.14:0.15:0.71. The discrepancy results mainly from the fact that the UGC aims at angular size completeness, thus favoring low surface brightness over compact galaxies (Haynes 1981) so that spirals and irregulars are preferred over E and S0. In addition, we expect that the present sample is contaminated by the presence of low-luminosity, preferentially spiral, foreground objects. A correction for this bias is attempted in the next section.

c) Biases and Subtraction of the Foreground Component

As mentioned in § IV*a*, we have chosen to derive the projected surface density σ from the CGCG, an apparent magnitude–limited sample, while galaxies with morphological types come from the UGC, a catalog which favors low surface brightness

objects over compact ones. Because galaxies at the two extremes of the surface brightness scale behave in opposite manners with respect to density, as shown in Figure 10, galaxies in the UGC will exhibit a marked preference for the low-density regions, in comparison with those included only in the CGCG. In Figure 11, the ratio of the number of galaxies in each catalog n(UGC)/n(CGCG) is plotted as a function of the surface density of galaxies for the Perseus region. While in cells of log $\sigma > 1.0$ that ratio hovers around 0.5, it rises dramatically in the low-density regions. The effect of this bias on the slope of the curves plotted in Figure 10 is twofold. First, if the surface density computation included the low surface brightness objects, the densities of the cells with lower values of σ would be increased, resulting in a restriction of the range of the abscissa in Figure 10. Second, if morphological types were available for all the CGCG galaxies, we expect that more of them would be high surface brightness, earlier type objects, located in higher density cells. Correction for both of these biases would result in a steepening of the population fraction curves shown in Figure 10 at both extremes of the morphological type range. An acceptably accurate knowledge of the type distribution of CGCG galaxies excluded from the UGC is not available. Hence, we refrain from attempting to correct for the catalog bias, but we note that such a correction would only dramatize the conclusions reached at the end of § IV*b*.

Figure 3 illustrates how the surface density obtained for a given volume density enhancement can depend on its distance from us. Intrinsically large and bright objects in dense but distant regions will fill bins of relatively low σ if their neighbors fall beyond the catalog limit. The effect of this bias will be similar to that discussed above, as a softening of the rise of the fraction f with increasing σ among the early types.

A potentially more worrisome bias, especially for the lowest luminosity galaxies included in the bin corresponding to column (9) of Table 2, derives from the fact that a larger fraction of those are nearby objects than are most early type galaxies. Because the density enhancements associated with the Perseus supercluster are more distant than a redshift of 3000 km s^{-1}, a nonnegligible population of foreground objects may affect the counts, especially for later morphologies. Because their probability of falling within a given cell of the density map is practically independent of σ, a population of foreground objects would have a steeply decreasing slope in Figure 10. This bias will of course affect all morphologies, but more strongly those with intrinsically fainter galaxies. We can roughly correct for this effect as follows. For each morphological type T, we construct a histogram of the velocity distribution of all galaxies with available redshift. A fraction $f(T)$ is assumed to be part of the foreground population if the velocity is smaller than 2000 km s^{-1}. Assuming that these foreground galaxies are randomly distributed, then we can correct the counts of the corresponding type at density σ, $n(T, \sigma)$, to a value

$$n'(T, \sigma) = n(T, \sigma) - f(T)n_c(\sigma)N(T)/M \ , \qquad (3)$$

where $n_c(\sigma)$ is the number of cells in the density map characterized by the density σ, $N(T)$ is the total number of galaxies of type T contained in the map (integrated over all densities, $\int n(T, \sigma)d\sigma$, and M is the total number of cells in the map.

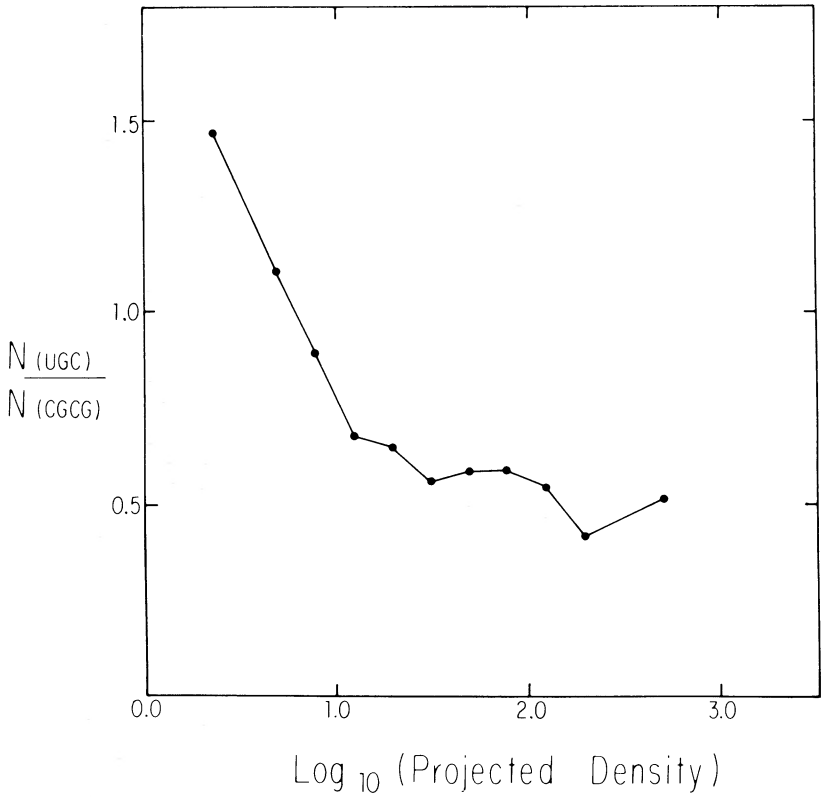

FIG. 11.—The ratio of the number of galaxies included in the UGC to the number of galaxies included in the CGCG as a function of the projected surface density of galaxies in the Perseus region. The density array is the same as that used to construct Fig. 1 and makes use of the CGCG.

TABLE 3

COUNTS OF UGC GALAXIES BY MORPHOLOGICAL TYPE CORRECTED FOR FOREGROUND CONTRIBUTIONS

log σ (1)	E (2)	S0, S0a (3)	Sa, Sab (4)	Sb (5)	Sbc (6)	Sc (7)	S... (8)	Later (9)	Sum (10)
0.2.....	0	0	3	5	2	11	7	9	37
0.6.....	7	19	17	26	17	55	43	45	229
1.0.....	19	91	51	91	44	184	133	134	747
1.4.....	58	141	116	135	74	234	190	150	1098
1.8.....	53	132	74	73	37	115	85	60	629
2.2.....	42	55	27	28	7	27	17	5	208
2.6.....	19	21	9	5	1	7	5	0	67
>2.8.....	5	3	1	1	0	1	0	0	11

Table 3 lists the corrected counts for each bin of morphological type, after subtraction of the foreground component. As anticipated, the largest values of $f(T)$ occur in column (9). Similar to Figure 10, Figure 12 shows the variation with density of the population fraction for different type subgroups in the Perseus region, but now after subtraction of the foreground component. The qualitative characteristics emphasized in Figure 10 remain in Figure 12.

V. DISCUSSION

While the current availability of three-dimensional data as well as our lack of understanding of the detailed structure of

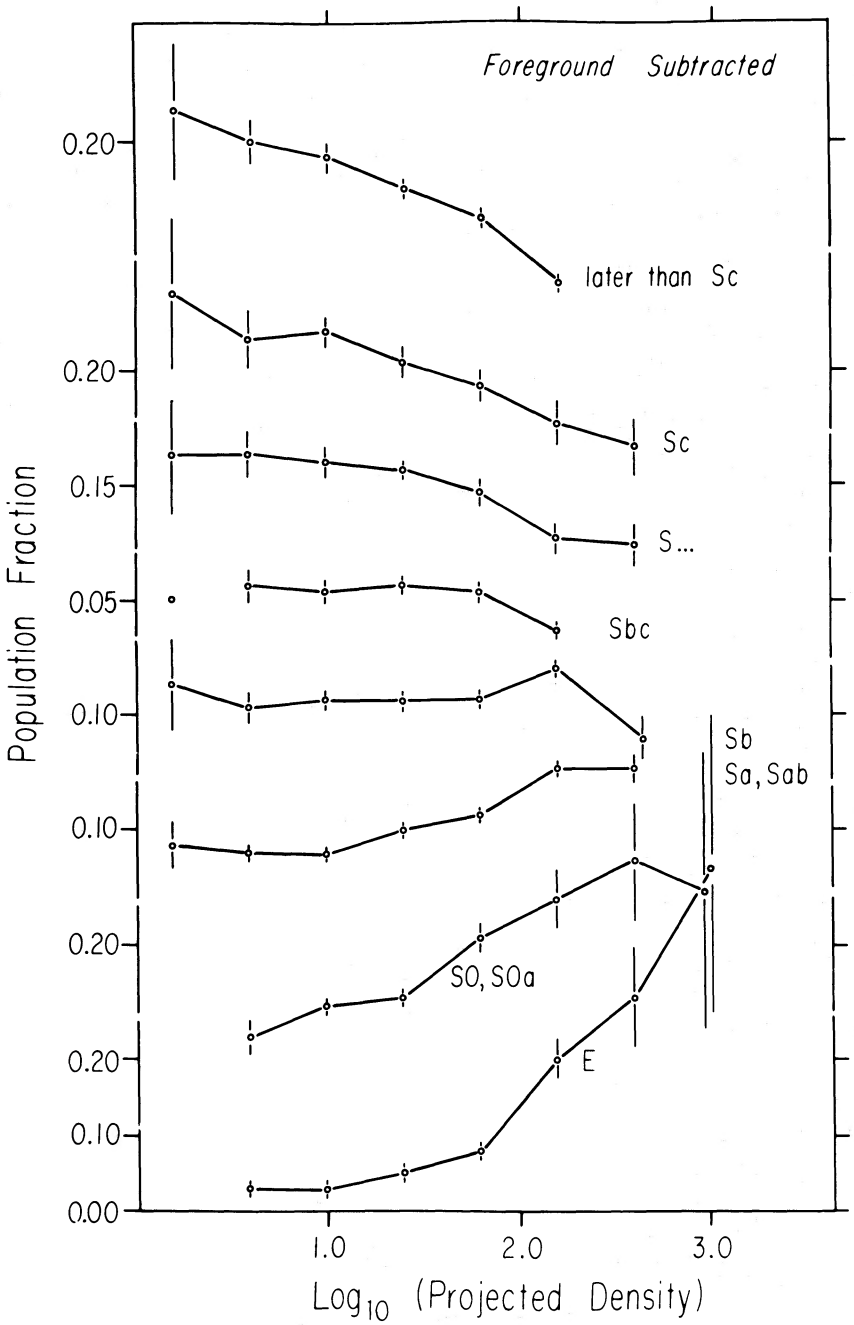

FIG. 12.—Similar to Fig. 10, but with the foreground component subtracted as discussed in the text

the large-scale distribution of galaxies does not permit a complete analysis of the morphological effects of volume density, the relative closeness and favorable viewing aspect of the Pisces-Perseus supercluster do allow a study of the consequential tendencies of morphological segregation. The existent data outline the gross structure of the supercluster and its limits. We have employed the present knowledge to investigate the variation of clustering properties of galaxies in different morphological type subgroups and the effect of local density on the segregation of galaxy classes within the range of densities representative of the supercluster structure. Our main conclusions are the following:

1. As shown in § II, the surface density enhancements seen in Figure 1 do indeed trace the volume density enhancements associated with the supercluster.

2. Similar to the results found for other samples (Davis and Geller 1976), early-type galaxies in the Pisces-Perseus region have steeper two-point angular correlation functions, and thus tend to cluster on smaller angular scales, than do the later type spirals and irregulars. In addition, however, the correlation function $w(\theta)$ for Sa and Sab galaxies in this region is significantly steeper than that found for Sb's or Sc's.

3. In agreement with the well-established trend seen in the rich clusters by Dressler (1980) and extended to groups by others (Bhavsar 1981; De Souza *et al.* 1982; Postman and Geller 1984), the population fractions of elliptical and S0 galaxies in Perseus grow with increasing density, while the corresponding spiral fraction decreases. In this supercluster, the variation in the population fractions can be traced smoothly to regions of very low density. For most morphological classes, a gradient in the population fraction is evident at nearly all density regimes. Furthermore, the progressive change in the population fraction with density varies among the spiral types. Even while the fraction of the total population which are classified as spirals decreases as the galaxian density grows, the relative proportion of spirals that are of type Sa and Sab increases, while that of Sbc's and Sc's is correspondingly reduced.

The analysis presented in the preceding sections suggests that a significant degree of morphological segregation exists over the wide range of volume densities characteristic of the Pisces-Perseus supercluster. The continuous variation in population fraction is traceable over scales which well exceed those of single groups and clusters of galaxies, and into density regimes well below those that characterize those high-density perturbations of the galaxy distribution. Furthermore, morphological segregation is not only limited to the three main categories of ellipticals, gas-poor disk systems (S0's), and gas-rich objects (spirals and irregulars), but is also seen to vary within the range of spiral types as well. The smooth change in the observed population fraction among the spiral types implies that the conditions that lead to the currently observed morphological distribution arise to a large extent from the matter density at the time of formation, or at least at an early phase of galaxy evolution.

Mechanisms for secular, environmentally driven galactic evolution have been shown to be possibly effective, and currently at work, in cluster cores (e.g., Giovanelli and Haynes 1985), but the regimes of density within which such processes could be of significance in enhancing the morphological segregation properties represent a very small fraction of the total volume of the universe (Dressler 1984). Such ongoing alterations affect only a small fraction of the galaxian population. Moreover, the presence of early-type systems in extremely low-density regions argues against the determination of their morphology by mergers or other recent interactions. While it may be reasonable to understand how to convert gas-rich spiral disks into gas-poor, or perhaps even lenticular, objects via ongoing gas removal mechanisms, it is less so to explain the regularity of the morphological segregation which runs through the Hubble sequence from dwarfs and irregulars all the way to ellipticals. The typical velocity dispersions measured in the filamentary structures in Perseus, away from the clusters and groups (see Fig. 4 [*lower*]), are quite small, on the order of 300 km s^{-1} or even less; diffusion of galaxies whose morphology is first determined in high-density cluster cores to the low-density regimes in which they are currently located is not a viable process over a Hubble time.

As pointed out by Oort (1983), the question of large-scale morphological segregation is relevant to the choice between "bottom-up" and "top-down" scenarios on the origin of galaxies and clusters (Zel'dovich, Einasto, and Shandarin 1982; Peebles 1984). If the initial perturbations first formed galaxies with subsequent formation of clusters and superclusters by dissipationless collapse (Dekel 1983; Peebles 1984), the explanation of morphological segregation must invoke environment-dependent mechanisms that are capable of altering drastically the evolution of galaxies in a much more density-sensitive manner than those currently active in cluster cores. If, on the other hand, large-scale perturbations collapsed first, the successive formation of galaxies of different types may be finely tuned by the density of the pregalactic material. As pointed out by Oort (1984), the size of the initial cloud necessary to produce a galaxy of given mass would vary in regions of different density, as would the endowed angular momentum. The latter property undoubtedly plays a role in determining a galaxy's morphology.

Good evidence has however been presented against a strictly "top-down" scenario. As noted in Dekel, West, and Aarseth (1984), a pure adiabatic spectrum of baryons or of massive neutrinos can reproduce the observed characteristics of the correlation function of the galaxian distribution only if large-scale structures (superclusters) collapsed at a relatively late era (at $z = 1$ or 2), presumably after galaxies themselves had formed. Those authors thus favor a hybrid picture, with galaxies forming before superclusters, and adiabatic perturbations corresponding to the latter collapsing in a dissipationless mode at relatively recent times. Such a description may be posed with the problem of explaining the morphological segregation seen on the supercluster scale proposed here. It is unlikely that currently popular mechanisms of merging and gas removal can account for the observed segregation over such wide ranges of density.

It is obvious that the results presented here are limited by the assumption of a surface density parameter as the independent variable in the analysis. Despite the favorable aspects of the study of this particular supercluster which allow the first-order analogy of surface and volume density enhancements, it is clear that systematic bootstrapping from one variable to the other will not be possible without a more complete redshift data base at hand. We look forward to the opportunity to be able soon to examine the true three-dimensional framework of the galaxian distribution in the region of the Pisces-Perseus supercluster.

We would like to thank J. Roth, S. Djorgovski, and A. Szalay for kindly providing us with a version of their correlation analysis program, and J. Huchra for allowing access to his redshift compilation. One of us (G. L. C.) received partial support for this research by NSF under grant AST-8200727.

REFERENCES

Bernheimer, W. E. 1932, *Nature*, **130**, 132.
Bhavsar, S. P. 1981, *Ap. J. (Letters)*, **246**, L5.
Burstein, D., and Heiles, C. 1978, *Ap. J.*, **225**, 40.
Chincarini, G. L. 1982, in *The Large Scale Structure of the Universe*, III Escola de Cosmologia e Gravitaçao (Rio de Janeiro: Observatorio Nacional), p. 12.
Chincarini, G. L., Giovanelli, R., and Haynes, M. P. 1983, *Astr. Ap.*, **121**, 5.
Davis, M., and Djorgovski, S. 1985, *Ap. J.*, **299**, 000.
Davis, M., and Geller, M. J. 1976, *Ap. J.*, **208**, 13.
Dekel, A. 1983, *Ap. J.*, **264**, 373.
Dekel, A., West, M. J., and Aarseth, S. J. 1984, *Ap. J.*, **279**, 1.
De Souza, R. E., Capelato, H. V., Arakaki, L., and Logullo, C. 1982, *Ap. J.*, **263**, 557.
De Souza, R. E., Vettolani, G., and Chincarini, G. L. 1985, *Astr. Ap.*, **143**, 143.
de Vaucouleurs, G. 1975, in *Galaxies and the Universe, Stars and Stellar Systems*, Vol. **9**, ed. A. Sandage, M. Sandage, and J. Kristian (Chicago: University of Chicago Press), p. 557.
Dressler, A. 1980, *Ap. J.*, **236**, 351.
———. 1984, *Ann. Rev. Astr. Ap.*, **22**, 185.
Einasto, J., Joeveer, M., and Saar, E. 1981, *M.N.R.A.S.*, **193**, 353.
Giovanelli, R. 1983, in *IAU Symposium 104, Early Evolution of the Universe and its Present Structure*, ed. G. O. Abell and G. L. Chincarini (Dordrecht: Reidel), p. 273.
Giovanelli, R., and Haynes, M. P. 1982, *A.J.*, **87**, 1355.
———. 1985, *Ap. J.*, **292**, 404.
Gregory, S. A., Thompson, L. A., and Tifft, W. G. 1981, *Ap. J.*, **243**, 411.
Haynes, M. P. 1981, *Ap. J. Suppl.*, **42**, 83.
Haynes, M. P., and Giovanelli, R. 1983, *Ap. J.*, **275**, 472.
Haynes, M. P., Giovanelli, R., and Chincarini, G. L. 1984, *Ann. Rev. Astr. Ap.*, **44**, 445.
Hewett, P. C. 1982, *M.N.R.A.S.*, **201**, 187.
Melnick, J., and Sargent, W. L. W. 1977, *Ap. J.*, **215**, 401.
Nilson, P. 1973, *Uppsala General Catalog*, *Uppsala Astr. Obs. Ann.*, **6** (UGC).
Oemler, A. 1974, *Ap. J.*, **194**, 1.
Oort, J. H. 1983, *Ann. Rev. Astr. Ap.*, **21**, 373.
———. 1984, in *Clusters and Groups of Galaxies*, ed. F. Mardirossian, G. Giuricin, and F. Mezzetti (Dordrecht: Reidel), p. 1.
Peebles, P. J. E. 1980, *Large Scale Structure of the Universe* (Princeton: Princeton University Press).
———. 1984, *Science*, **224**, 1385.
Postman, M., and Geller, M. J. 1984, *Ap. J.*, **281**, 95.
Sandage, A., and Tammann, G. 1981, *Revised Shapley Ames Catalog* (Washington: Carnegie Institution).
Schechter, P. 1976, *Ap. J.*, **203**, 297.
Zel'dovich, Ya. B., Einasto, J., and Shandarin, S. F. 1982, *Nature*, **300**, 407.
Zwicky, F., Herzog, E., Karpowicz, M., Kowal, C. T., and Wild, P. 1961–1968, *Catalog of Galaxies and Clusters of Galaxies*, 6 vols. (Pasadena: California Institute of Technology Press), (CGCG).

G. L. CHINCARINI: European Southern Observatory, Karl-Scharzschild-Str. 2, D-8046 Garching bei München, Federal Republic of Germany

RICCARDO GIOVANELLI: Arecibo Observatory, P.O. Box 995, Arecibo, PR 00613

MARTHA P. HAYNES: Department of Astronomy, Cornell University, Ithaca, NY 14853